THE CRYSTALLOGRAPHY OF MARTENSITE TRANSFORMATIONS III. FACE-CENTRED CUBIC TO BODY-CENTRED TETRAGONAL TRANSFORMATIONS*

J. S. BOWLES and J. K. MACKENZIE†

The theory developed in Parts I and II is applied to transformations from face-centred cubic to body-centred tetragonal in the alloys Fe-C, Fe-Ni, Fe-Ni-C. The theoretical predictions of habit planes, orientation relationships and directions of the homogeneous strain are found to be in satisfactory agreement with all the available experimental data. Thus, the hypothesis that the inhomogeneous shear is a part of the twinning shear in the final structure has been substantiated for the transformations considered.

The habit plane interface envisaged by Frank is shown to be a special case of the type of interface expected on the present theory: all planes in the zone of the invariant line, and in particular the twinning plane, meet edge to edge in the interface.

LA CRISTALLOGRAPHIE DES TRANSFORMATIONS MARTENSITIQUES III. LES TRANSFORMATIONS DU SYSTÈME CUBIQUE À FACES CENTRÉES EN TÉTRAGONAL CENTRÉ

La théorie développée dans les Parties I et II est appliquée aux transformations du système cubique à faces centrées en tétragonal centré, dans les alliages Fe-C, Fe-Ni, Fe-Ni-C. Il est constaté que les prédictions théoriques des plans limites, des relations d'orientation et des directions de déformation homogène sont en accord satisfaisant avec toutes les données expérimentales, disponibles. Ainsi, l'hypothèse que la tension non-homogène fait partie de la tension de maclage dans la structure finale, a été confirmée pour le cas des transformations considérées. Il est montré que l'interface constituée par un plan limite, envisagée par Frank, n'est qu'un cas particulier de l'interface proposée par la présente théorie, à savoir: tous les plans dans la zone de la ligne invariante, et en particulier le plan de maclage, se rencontrent suivant une arête commune dans l'interface.

DIE KRISTALLOGRAPHIE DER MARTENSIT TRANSFORMATIONEN. III. TRANSFORMATIONEN VON KUBISCH-FLÄCHENZENTRIERTEN ZU TETRAGONAL-RAUMZENTRIERTEN GITTERN

Die in Teil I und II entwickelte Theorie wird auf die Umwandlungen kubisch-flächenzentriert zu tetragonal-raumzentriert in Fe-C, Fe-Ni und Fe-Ni-C Legierungen angewandt. Die theoretischen Voraussagen über Habitusebenen, Beziehungen der kristallographischen Orientierungen und Richtungen homogener Verzerrungen stimmten zufriedenstellend mit allen vorhandenen experimentellen Angaben überein. Somit ist die Hypothese, dass die inhomogene Scherung einen Teil der Zwillingsscherung in der Endstruktur darstellt, für die hier betrachteten Transformationen bestärkt worden.

Es wird gezeigt, dass die von Franck vorgeschlagene Habitusebenengrenzfläche ein Spezialfall des nach der vorstehenden Theorie zu erwartenden Grenzflächentyps ist. Alle Ebenen in der Zone der invarianten Richtung und im besonderen die Zwillingsebene schneiden sich in der Grenzfläche.

1. Introduction

In this paper the geometrical theory of martensite transformations which was developed in Parts I and II‡ [1] will be applied to transformations from face-centred cubic to body-centred tetragonal lattices, and its predictions of habit planes, orientation relationships and other geometrical features will be compared with the available experimental data for iron-carbon, iron-nickel and iron-nickel-carbon alloys.

In I and II a phenomenological theory of the relations between the various crystallographic features of martensite transformations was developed. This theory aims at describing the total atomic displacements produced by martensite transformations but not necessarily the motions of atoms during transformation. It has been shown that the total atomic displacements can be described consistently by means of a homogeneous strain which is composed of an invariant-plane strain on the habit plane and a small dilatation, followed by an inhomogeneous shear which produces no further observable change in shape. This shear can only be homogeneous within small volumes and it was proposed that within such volumes it is a part of a twinning shear in the final lattice. It has been shown that these conditions, together with a knowledge of the correspondence between the two lattices, their dimensions, and the twinning plane involved, is sufficient to determine the total strain in terms of a single parameter, θ, and, further, that the resolution of this total strain into component strains of the required types is uniquely determined.

In §§2, 3, of the present paper the correspondence between the initial and final lattices, and also the relevant twinning plane, are shown to be

*Received September 5, 1953.

†Division of Tribophysics, University of Melbourne, Victoria, Australia.

‡These papers will be referred to as I and II.

the same for all the transformations considered. In these sections the experimental origins of this information are described and quantities which are required for direct substitution into the equations of the theory are derived. In §4 the parameter θ is introduced and substitution into the main equations of the general theory is carried out. To apply the theory to a particular transformation it is necessary to find the appropriate value of θ by calculating the variation of the habit plane with θ and determining that value for which the predicted and observed habit planes agree. Of course the extent to which there is agreement between the observed and the theoretically possible habit planes is a first test of the hypothesis that the inhomogeneous shear is a part of a twinning shear. The actual comparisons of predicted and observed habit planes are carried out in §5 and the appropriate values of θ are determined for the various transformations. The remaining sections of the paper are concerned with detailed analyses of individual transformations and show that the predictions of the theory are in substantial agreement with experiment.

The notation used in this paper is the same as that used in I and II.

2. The Correspondence and the Principal Axes

Jaswon and Wheeler [2] have determined the correspondence between *f.c.c.* and *b.c.t.* lattices for those transformations in iron-carbon alloys which produce the Kurdjumow-Sachs orientation relationship [3]. For the variant of this relationship shown in Figure 1, their correspondence is

$$(\mathrm{B}\mathbf{C}\mathrm{F}) = \begin{pmatrix} 1 & 0 & 1 \\ 1 & 0 & \bar{1} \\ 0 & 1 & 0 \end{pmatrix}, \tag{2.1}$$

where the bases B and F define the *b.c.t.* and *f.c.c.* unit cells respectively; the corresponding metrics* are $(\mathrm{B}^*\mathbf{G}\mathrm{B}) = (\text{diag: } a'^2, a'^2, \gamma^2 a'^2)$ and $(\mathrm{F}^*\mathbf{G}\mathrm{F}) = (\text{diag: } a^2, a^2, a^2)$ where a' and a are the respective lattice parameters and γ is the axial ratio of the tetragonal cell. This correspondence was chosen by Jaswon and Wheeler because it ensures that the atomic displacements involved in the transformation are as small as possible. It has been shown [4; 2] that the arrangement of interstitial carbon atoms in iron-carbon martensite is precisely that expected from this correspondence. It has also been shown [5] that the same correspondence results from a consideration of the analogous variants of all orientation relationships between Nishiyama [6] and Kurdjumow-Sachs, including that of Greninger and Troiano [7].

*The notation (diag: a, b, c) represents a square diagonal matrix with elements a, b, c in the leading diagonal, all other elements being zero.

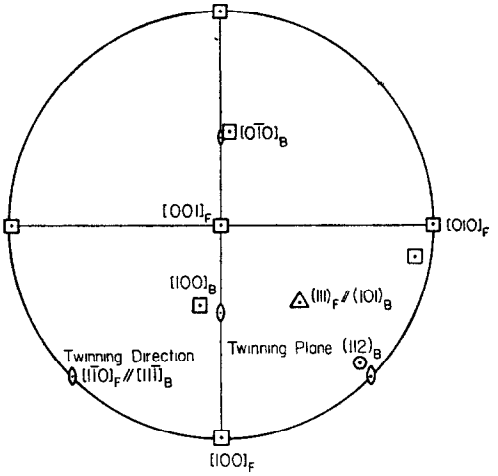

FIGURE 1. Stereographic projection showing the variant of the Kurdjumow-Sachs orientation relationship considered in this paper. The relevant twinning plane and twinning direction are also shown. The subscripts F and B refer to the f.c.c. and b.c.t. lattices respectively.

The correspondence and the metrics of the two bases B and F determine the principal axes, and the associated principal strains of the total strain, as described in II-§ 4. In the present case the results are easily obtained by inspection, for the mutually orthogonal directions $[101]_F$, $[10\bar{1}]_F$, $[010]_F$ correspond to the mutually orthogonal directions $[100]_B$, $[010]_B$, $[001]_B$. The former set of directions can therefore be chosen as principal axes and the basis P, comprised of unit vectors in these directions (Figure 2) defined to be $[\mathrm{F}; \mathbf{p}_1] =$

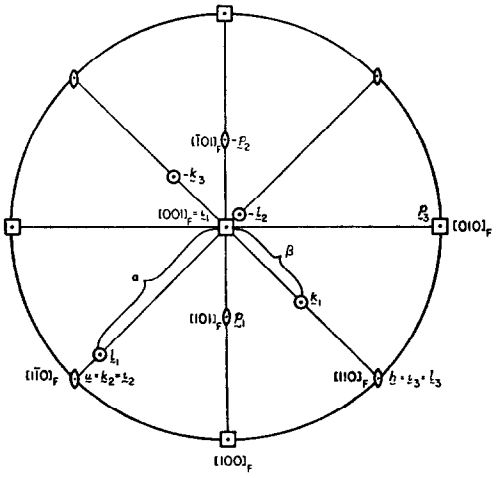

FIGURE 2. Stereographic projection showing the orientation of the bases P, I, L, K relative to the f.c.c. lattice. The invariant line and the invariant normal make angles α and β respectively with $[001]_F$.

$[1/\sqrt{2}, 0, 1/\sqrt{2}]_F$, $[F; \mathbf{p}_2] = [1/\sqrt{2}, 0, -1/\sqrt{2}]_F$, $[F; \mathbf{p}_3] = [0, 1, 0]_F$.
Thus,

$$(2.2) \qquad (P\mathbf{T}F) = \begin{pmatrix} 1/\sqrt{2}, & 0, & 1/\sqrt{2} \\ 1/\sqrt{2}, & 0, & -1/\sqrt{2} \\ 0 & , 1, & 0 \end{pmatrix} = (F\mathbf{T}P)'.$$

The elements of the diagonal matrix $\mathbf{M}$, representing the strain referred to the basis P which extends the base vectors P to their final lengths without rotation, are simply the ratios of the final to the initial identity periods along the principal axes. Thus,

$$(2.3) \qquad \mathbf{M}^2 = (a'/a)^2 \,(\text{diag: } 2, 2, \gamma^2).$$

3. The Twinning Plane and Direction

Greninger and Troiano [7] have observed twinned martensite plates in an iron-22% nickel-0.8% carbon alloy and have determined the indices of the twinning plane. Examination of their pole figure shows that the operative twinning plane is $(112)_B$ for the variant being considered in this paper.

That the twinning plane is the same for transformations which lead to the Kurdjumow-Sachs orientation relationship can be shown as follows. This orientation has the property that its variants are twin-related in pairs. The twinning shear relating such a pair variants can be obtained by stereographic analysis [5] making use of the correspondences for these variants. The relevant twinning plane is again found to be $(112)_B$ and the associated twinning direction is $[11\bar{1}]_B$. This twinning direction is the same as that obtained from the general equation for the twinning shear, II-(7.7), which gives

$$(3.1) \qquad (B\mathbf{S}^T B) = \mathbf{I} - f[1, 1, \bar{1}](1, 1, 2),$$

where $f = (2 - \gamma^2)/2(\gamma^2 + 2)$.

The intermediate basis I used in the general theory can now be determined explicitly. The base vector $\mathbf{i}_2 (= \mathbf{u})$ is a unit vector parallel to the direction in the initial lattice from which the twinning direction is generated. The base vector $\mathbf{i}_3 (= \mathbf{h})$ is a unit vector normal to the plane from which the twinning plane is generated, while $\mathbf{i}_1$ is a unit vector perpendicular to both. Using the correspondence (2.1) it follows that the twinning direction $[11\bar{1}]_B$ is generated from the direction $(B\mathbf{C}F)^{-1}[11\bar{1}]_B = [2\,\bar{2}\,0]_F$, so that $[F; \mathbf{i}_2] = [1/\sqrt{2}, -1/\sqrt{2}, 0]_F$. Similarly, the twinning plane $(112)_B$ is generated from the plane $(112)_B(B\mathbf{C}F) = (220)_F$ so that $[F; \mathbf{i}_3] = [1/\sqrt{2}, 1/\sqrt{2}, 0]_F$ and $[F; \mathbf{i}_1] = [0, 0, 1]_F$. These base vectors are shown in Figure 2. Finally, using (2.2) to transform the components of these base vectors to the basis P it follows that the transformation

$$(3.2) \quad (P\mathbf{T}I) = \begin{pmatrix} 1/\sqrt{2}, & 1/2, & 1/2 \\ -1/\sqrt{2}, & 1/2, & 1/2 \\ 0 & , -1/\sqrt{2}, & 1/\sqrt{2} \end{pmatrix} = (I\mathbf{T}P)'.$$

It should be noted that the twinning plane $(112)_B$ is generated from a plane of symmetry $(110)_F$ as required by the general theory, II-§ 7.

4. The Invariant Line Strain

The invariant line strain $\mathbf{S}$ that is obtained from the total strain $\mathbf{S}_t$ by removing a suitable dilatation $\mathbf{I}/\delta$, is calculated in II-§§6, 9 and is expressed ultimately in terms of the elements g_{rs} of a matrix.

$$(4.1) \qquad \mathbf{G} = (I\mathbf{T}P)\,\delta^2\mathbf{M}^2(P\mathbf{T}I).$$

The dilatation δ is the only unknown quantity in this equation, and is therefore the only adjustable parameter in the theory. However, δ itself is not the most convenient parameter to use. Equation (2.3) shows that $\delta^2\mathbf{M}^2 = \delta^2(a'/a)^2\,\mathbf{M}_0^2$, where $\mathbf{M}_0^2 = (\text{diag: } 2, 2, \gamma^2)$, which for a fixed γ is independent of the sizes of the initial and the final cells. Thus, if a new parameter θ is defined by the relation

$$(4.2) \qquad \theta = \delta(a'/a),$$

all transformations with the same γ can be treated simultaneously for they differ only with respect to the value of θ. In terms of the parameter θ

$$(4.3) \quad \mathbf{G} = (g_{rs}) = \theta^2 \begin{pmatrix} 2, 0 & , & 0 \\ 0, 1 + \gamma^2/2, & 1 - \gamma^2/2 \\ 0, 1 - \gamma^2/2, & 1 + \gamma^2/2 \end{pmatrix},$$

$$(4.4) \quad \mathbf{G}^{-1} = (g^*_{rs}) = \frac{1}{\theta^2} \begin{pmatrix} \frac{1}{2}, & 0 & , & 0 \\ 0, & (2 + \gamma^2)/4\gamma^2, & (\gamma^2 - 2)/4\gamma^2 \\ 0, & (\gamma^2 - 2)/4\gamma^2, & (2 + \gamma^2)/4\gamma^2 \end{pmatrix},$$

and

$$(4.5) \qquad |\mathbf{G}| = g^2 = 4\gamma^2\theta^6.$$

In II it was shown that the matrix representing the invariant line strain $\mathbf{S}$ has a simple form when referred to a basis L, such that $\mathbf{l}_1$ is parallel to the invariant line. The base vectors $\mathbf{l}_1$, $\mathbf{l}_2$, $\mathbf{l}_3$ are shown in Figure 2. The transformation

$$(4.6) \quad (I\mathbf{T}L) = \begin{pmatrix} \cos\alpha, & -\sin\alpha, & 0 \\ \sin\alpha, & \cos\alpha, & 0 \\ 0 & , 0 & , 1 \end{pmatrix},$$

where $\alpha(|\alpha| \leqslant 90°)$ is the angle between $\mathbf{l}_1$ and $[001]_F = \mathbf{i}_1$, and is determined by equation II-(6.10). On substituting the g_{rs} given in (4.3) into this equation it is found that

$$(4.7)\quad \cos\alpha = (1 - \theta^2 - \theta^2\gamma^2/2)^{\frac{1}{2}}/\theta(1 - \gamma^2/2)^{\frac{1}{2}},$$

$$(4.8)\quad \sin\alpha = (2\theta^2 - 1)^{\frac{1}{2}}/\theta(1 - \gamma^2/2)^{\frac{1}{2}},$$

giving two values of α which are merely opposite in sign. It should be noted that these equations only determine real values of α provided $1/\sqrt{2} \leqslant \theta \leqslant 1/(1 + \gamma^2/2)^{\frac{1}{2}}$, thus imposing limits on the possible values of θ; the minimum and maximum values of θ correspond to $\alpha = 0°$ and $90°$ respectively.

The matrix representing $\mathbf{S}$ referred to the basis L is given by II-(8.7), (6.18)

$$(4.9)\quad (\mathrm{L}\mathbf{S}\mathrm{L}) = \begin{pmatrix} 1, & (g_{22} - g_{11})\cos\alpha\sin\alpha, & g_{23}\sin\alpha \\ 0, & g g_{33}^{*\frac{1}{2}}\cos\omega, & -(g g_{23}^{*\frac{1}{2}}\cos\alpha\cos\omega + \sin\omega)/g_{33}^{*\frac{1}{2}} \\ 0, & g g_{33}^{*\frac{1}{2}}\sin\omega, & (-g g_{23}^{*\frac{1}{2}}\cos\alpha\sin\omega + \cos\omega)/g_{33}^{*\frac{1}{2}} \end{pmatrix},$$

where ω is the angle between the initial and final positions of the twinning plane and is found from II-(8.5) to be

$$(4.10)\quad \cos\omega = (2\theta\gamma + 1 + \gamma^2/2)/(1 + \theta\gamma)(2+\gamma^2)^{\frac{1}{2}},$$

giving two values of ω, opposite in sign. It should be noted that $\cos\omega$ must be positive since the criterion for selecting the correspondence ensures that the total strain is as small as possible: if $\cos\omega$ were negative the twinning plane would have to be rotated by more than $90°$ by the transformation. Considerations such as this show that all the square roots must be taken positively unless the contrary is stated.

The two values of α taken together with the two for ω determine four possible invariant line strains, all of which have the same principal axes and associated principal strains, and the twinning plane is generated from the same plane $(110)_F$ in all four cases. The solution obtained by taking α and ω both positive, say, will be referred to as the $(\alpha+, \omega+)$-solution and so on. In II-§ 8, it was shown that the $(\alpha+, \omega-)$-solution refers to the twin of that variant of the $(\alpha+, \omega+)$-solution which is obtained by a rotation of 180° about the normal to the $(110)_F$ symmetry plane. The $(\alpha-, \omega-)$- and the $(\alpha-, \omega+)$-solutions are related in the same way. In general, the $(\alpha+, \omega+)$- and $(\alpha-, \omega+)$-solutions are distinct, but in the present case they are variants related by a rotation through 180° about the normal to the $(001)_F$ symmetry plane. The other pair are, of course, related in the same way. Examination of Figure 2 shows that this symmetry operation leaves the principal axes, principal strains and the plane $(110)_F$ invariant* while it changes $\mathbf{l}_1(\alpha+)$ into $\mathbf{l}_1(\alpha-)$. This result can be demonstrated formally by showing that the $(\alpha-, \omega+)$-solution, when referred to the variant of its L basis, is identical with the $(\alpha+, \omega+)$-solution.

The factorization of $\mathbf{S}$ can now be carried out making use of the relations given in II-§ 9. In the present class of transformations certain simplifications arise and the formulae can be given geometrical interpretations which are sometimes useful. For the $(\alpha+, \omega+)$-solution, unit vectors along the normal to the habit plane and in the direction of the displacement in the invariant plane strain are given by

$$(4.11)\quad \left.\begin{aligned} (\mathbf{p};\ \mathrm{L}) &= (0, -1, \cos\beta)_{\mathrm{L}}/(1 + \cos^2\beta)^{\frac{1}{2}}, \\ (\mathbf{p};\ \mathrm{I}) &= (\sin\alpha, -\cos\alpha, \cos\beta)_{\mathrm{I}}/(1+\cos^2\beta)^{\frac{1}{2}}, \end{aligned}\right\}$$

$$(4.12)\quad \left.\begin{aligned} [\mathrm{K};\ \mathbf{d}] &= [0, \cos\alpha, -1]_{\mathrm{K}}/(1 + \cos^2\alpha)^{\frac{1}{2}}, \\ [\mathrm{I};\ \mathbf{d}] &= [\sin\beta, \cos\alpha, -\cos\beta]_{\mathrm{I}}/(1+\cos^2\alpha)^{\frac{1}{2}}, \end{aligned}\right\}$$

where K is the basis introduced at the end of II-§6 and β, the angle between $[100]_{\mathrm{I}}$ and the invariant normal of $\mathbf{S}$, is given by II-(6.11)

$$(4.13)\qquad \sin\beta = \sqrt{2}\gamma(2\theta^2 - 1)^{\frac{1}{2}}/(2 - \gamma^2)^{\frac{1}{2}}.$$

It follows from (4.11) that for constant β the habit plane is a fixed plane in the L-basis. Since the L-basis only varies by a rotation about $[110]_F$, the normal to the habit plane varies in the same way for constant β. Similarly for constant α the direction only varies by a rotation about $[1\bar{1}0]_F$. Further, the magnitude m (I-§5) of the invariant plane strain reduces to

$$(4.14)\qquad m = \sqrt{2}\,\theta(1 - \theta\gamma),$$

while the fraction k of the twinning shear involved in the complementary strain is given by

$$(4.15)\qquad 1 + 2k = \cos\alpha\cos\beta.$$

*Since $[001]_F$ is a line of symmetry in the initial position of the twinning plane $(110)_F$, these facts show that the two possible values of α can differ only in sign.

5. The Habit Plane

It was shown in II-(9.3) that the habit plane referred to the basis L is of the form $(0, \sin\omega, g_{33}^{*-\frac{1}{2}} - \cos\omega)_L$. On substituting for ω and g_{33}^* this becomes

$$(5.1)\quad (0,\ \mathrm{sgn}\ \omega\ (1-\gamma^2/2)^{\frac{1}{2}},\ -[1-\gamma^2(4\theta^2-1)/2]^{\frac{1}{2}})_L.$$

The habit plane can now be referred to the basis F using the transformation

$$(\mathrm{FT_L}) = (\mathrm{FT_P})(\mathrm{PT_I})(\mathrm{IT_L}),$$

$$(5.2)\qquad = \begin{pmatrix} \sin\alpha/\sqrt{2}, & \cos\alpha/\sqrt{2}, & 1/\sqrt{2} \\ -\sin\alpha/\sqrt{2}, & -\cos\alpha/\sqrt{2}, & 1/\sqrt{2} \\ \cos\alpha & -\sin\alpha, & 0 \end{pmatrix}.$$

The variation of the habit plane with θ for $\gamma = 1$, i.e., for body-centred cubic structures, is shown in Figure 3 for all four solutions, and the relationship between the solutions is clearly that described previously. Since the four habit planes are crystallographically equivalent, it is only necessary to consider one eighth of the whole projection in order to compare experimental habit planes with those predicted by the theory. Accordingly, in Figure 4 the variation of the habit plane with θ and γ has been plotted for the $(\alpha+, \omega+)$-solution.

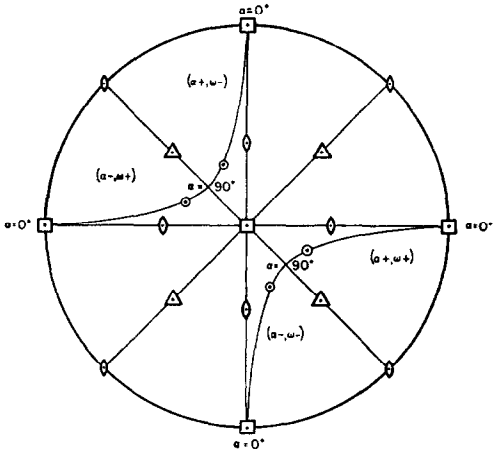

FIGURE 3. Stereographic projection showing the variation of the habit plane with θ for $\gamma = 1$. As θ^2 varies between the limits 1/2 and 2/3, α varies from 0 to 90 degrees. The open circles represent the four solutions obtained for the habit plane for some particular value of θ.

The compositions of those alloys for which habit planes have been determined are given in Table I, which also shows the corresponding values of γ and $(a'/a)^2$. In all the experimental work, with one exception [7] only the general indices of the habit plane have been determined. In

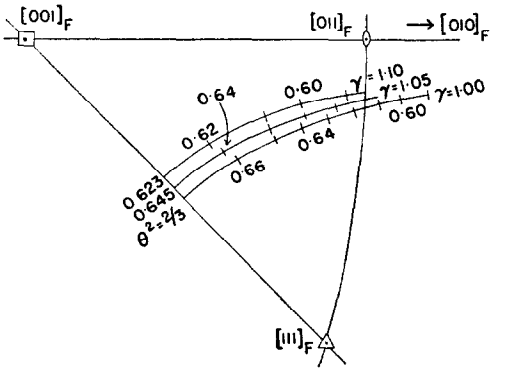

FIGURE 4. Stereographic projection showing the variation of the habit plane with θ and γ.

Figures 5, 6, 7, where the measured habit planes are compared with the theory, the experimental habit planes have been plotted in the stereographic triangle containing the predicted curves. It will be shown in the next section that Greninger and Troiano's habit plane does indeed lie in this triangle.

It is evident from these diagrams that the experimental results are in general agreement with the theory. The observed habit planes lie close to the calculated curves for the relevant γ, and the predicted lateral shift of the habit plane curves as γ increases is in good agreement with observation (Figure 5).

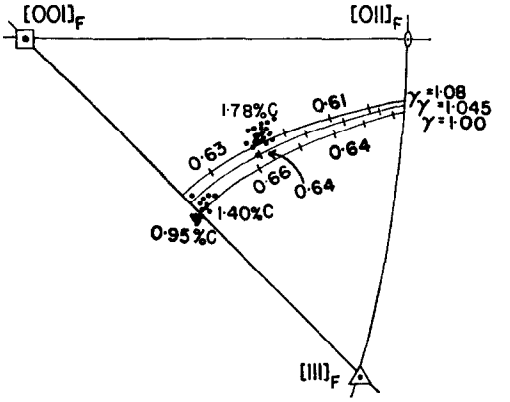

FIGURE 5. Comparison of the predicted habit planes with those measured by Greninger and Troiano [7] for various iron-carbon alloys. Following Greninger and Troiano, the results for 0.95%C. have been plotted in the adjoining triangle. According to the theory each group of points should lie somewhere on the curve for the appropriate γ.

The exact location of a habit plane on a particular curve is determined by the value of the parameter $\theta = \delta a'/a$. Although the exact values of δ are not known, they must be close to unity (I-§4). Thus, by regarding θ as equal to a'/a, a crude comparison of the predicted with the observed

effects of varying θ can be made. The theory then predicts that a'/a decreases either as γ increases or as the habit plane is displaced along a curve towards $(010)_F$. Examination of the data in Table I shows that a'/a always decreases as γ increases. Furthermore, in those transformations for which $\gamma = 1$ (Fig. 7) and also in those for which $\gamma = 1.041$, 1.045 (Fig. 6) the habit plane moves in

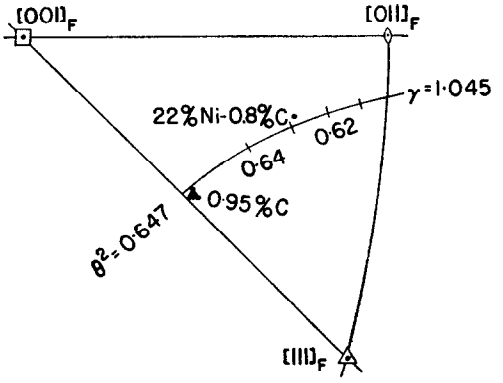

FIGURE 6. Comparison of the predicted and measured habit planes for transformations with $\gamma \simeq 1.045$.

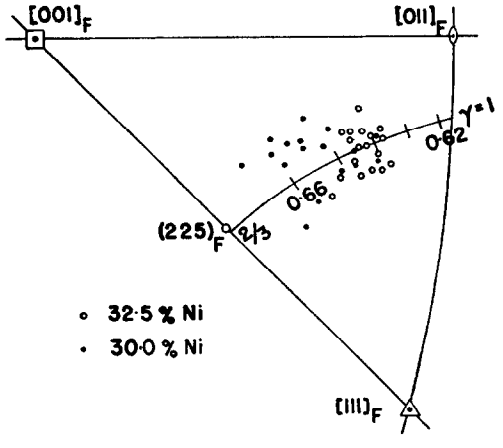

FIGURE 7. Comparison of the predicted and measured habit planes for transformations with $\gamma = 1$. The results for 30.0% and 32.5% Ni are those obtained respectively by Machlin and Cohen [14] and Greninger and Troiano [7].

the predicted direction as a'/a varies. Thus, the theory accounts for the general trends of habit plane variation. Quantitative agreement is achieved by evaluating the adjustable parameter δ.

The values of θ^2 which lead to the best agreement with the experimental habit planes have been estimated for each transformation, and are given in Table I, together with the values of δ derived therefrom. The values of δ are all within 1.5% of unity, in agreement with the observational evidence that any dilatation of the habit plane could not exceed a few per cent. (I-§4).

The feature of the experimental data that seems

TABLE I

Composition	γ	$(a'/a)^2$	θ^2	$\delta = \theta a/a'$	References
Carbon Steels					
0 %C.	1.000	0.650	0.6667†	1.013	
0.35%C.	1.016	0.642	0.6596†	1.014	
0.92%C.	1.041	0.630	0.6481†	1.014	Roberts* [8]
1.40%C.	1.063	0.620	0.6386†	1.015	
1.78%C.	1.080	0.612	0.620	1.006	
Fe–30% Ni	1.000	0.642	0.647‡	1.004‡	Owen, Yates and Sully [9]; Bradley,
Fe–32.5%Ni	1.000	0.640	0.645	1.004	JayandTaylor[10]; Jette and Foote [11]; Phragmen; [12]; Nishiyama [6].
Fe–0.8%C. –22%Ni	1.045	0.627	0.630	1.002	Greninger and Troiano [7].

*For Fe–C alloys Roberts summarises all the existing data and gives $a = (3.548 + 0.044x)kX$, $a' = (2.861 - 0.013x)kX$, $\gamma = 1.000 + 0.045x$, where x is the wt. % carbon. For pure iron, Barrett [13] gives $a = 3.564\text{Å} = 3.557kX$ differing from Roberts' extrapolated value and obtained by extrapolation of high-temperature data.

†$\theta^2 = 1/(1 + \gamma^2/2) = \theta^2_{max}$.

‡The wide scatter of the observed habit planes makes it difficult to estimate θ^2. The value given has been obtained by assuming $\delta = 1.004$ (as for Fe–32.5% Ni) and using the value of $(a'/a)^2$ to calculate θ^2. The theoretical habit plane for $\theta^2 = 0.647$ lies within the scatter of the observations.

most difficult to reconcile with the theory is the wide scatter of the observed habit planes, particularly in the iron-nickel alloys (Fig. 7). Since it seems unlikely that the whole of this scatter can be due to experimental error other possibilities must be considered. The scatter parallel to the predicted curves could, of course, be attributed to variations in θ from plate to plate. Such variations could arise from changes in δ and/or a'/a due to inhomogeneneity of composition. The scatter normal to the predicted curves cannot be explained in this way, and, if it is a true effect, it may be necessary to abandon the hypothesis that the complementary shear occurs on the twinning plane and in the twinning direction and examine the consequences of fulfilling only one of these conditions (I-§§6, 9). However, it is clear that all the general features of habit plane variation are accounted for satisfactorily by the present hypothesis, and in the remaining sections it will be shown that by using the values of θ determined above, other crystallographic features of the transformations can also be accounted for quantitatively.

6. Greninger and Troiano's (259)-Transformation

The most complete experimental analysis of a martensite transformation is that made by Grenin-

ger and Troiano [7] of the transformation in Fe–0.8% C–22% Ni. They determined the habit plane and orientation relationship for a particular variant and also the direction of the homogeneous strain, assuming this strain to be a simple shear on the habit plane. The predictions of the theory for this transformation will now be compared with their observations.

It is clear from Figure 6 that the predicted and experimental habit planes are in good agreement for $\gamma = 1.045$, if $\theta^2 = 0.63$. Of the four possible strain matrices which can now be obtained using these values it is only necessary to consider any two which characterise a parent and a variant of its twin; the other two solutions are just real variants of these. A suitable pair is the $(\alpha+, \omega+)$- and the $(\alpha+, \omega-)$-solutions, and of these it is the $(\alpha+, \omega+)$-solution which leads to agreement with Greninger and Troiano's orientation relationship. For this transformation $\alpha = 72° 26.87'$ and $\omega = 4° 57.30'$ and the $(\alpha+, \omega+)$-solution* is

$$(6.1) \qquad (\text{LSL}) = \begin{pmatrix} 1, & -0.082238, & 0.272696 \\ 0, & 1.103662, & 0.016254 \\ 0, & 0.095683, & 0.948345 \end{pmatrix},$$

while the transformation (FTL) is obtained from equation (5.2) with $\sin\alpha = 0.953443$ and $\cos\alpha = 0.301574$.

The relative orientation of the two lattices can now be found very simply, for the indices, relative to the basis F, of any direction $[u\,v\,w]_B$ are (FSF)(FCB)$[u\,v\,w]_B$ while a plane $(hkl)_B$ has indices $(hkl)_B$(BCF)(FSF)$^{-1}$ relative to F. In Table II the

TABLE II

COMPARISON OF PREDICTED AND MEASURED ORIENTATION RELATIONSHIPS IN FE–22% NI–0.8% C.

Corresponding directions	Measured angle	Predicted angle
$[1\bar{1}0]_F$—$[11\bar{1}]_B$	2.5°	2.7°
$[0\bar{1}1]_F$—$[1\bar{1}\bar{1}]_B$	6.5°	6.6°
$[1\bar{2}1]_F$—$[10\bar{1}]_B$	2.0°	1.9°
$(111)_F$—$(101)_B$	about 1°	0.2°

predicted angles between various corresponding directions and planes are compared with those measured by Greninger and Troiano [7; Figs. 3 and 6]. It is evident that the two sets of angles are in very good agreement. The greatest discrepancy (0.8°) is in the angle between $(111)_F$ and $(101)_B$ but this is of doubtful significance since it is not indicated in Greninger and Troiano's paper whether the angle was measured directly or obtained by graphical construction. Since a gnomonic projection was used the latter possibility seems the more likely, and in this case the discrepancy is not surprising. Notwithstanding its magnitude, the predicted displacement of the $(101)_B$-pole from the $(111)_F$-pole is, as far as can be judged, in the observed direction. The other three angles appear to have been rounded off and the values given are, in fact, inconsistent with a tetragonal structure with $\gamma = 1.045$. (The results imply an angle of not more than 69.0° between $[1\bar{1}\bar{1}]_B$ and $[11\bar{1}]_B$ whereas the correct angle is 69.3°). Thus, the small discrepancies in these three angles may be even further reduced, and since these three angles define the fourth, the estimate of 1° may need some amendment.

For this transformation the theory not only predicts the observed orientation relationship but also the observed orientation of the habit plane relative to both lattices. It is readily demonstrated that a pole figure showing the austenite axes, the predicted martensite axes and habit plane, can be rotated into coincidence with the pole figure determined by Greninger and Troiano [7; Fig. 6]. The theory, therefore, predicts the correct habit plane: not merely a plane of the correct form.

The orientation relationship derived from the $(\alpha+, \omega-)$-solution is simply a variant of the $(112)_B$-twin of the orientation just considered. Greninger and Troiano have observed twins on this plane so that all orientations predicted by the theory actually occur. However, the reported orientation is produced in preference to its twin. A rational explanation of this observation becomes apparent on carrying out the factorization into component strains of both the $(\alpha+, \omega+)$- and the $(\alpha+, \omega-)$-solutions. The homogeneous strains are, of course, variants of the same strain, while the inhomogeneous strains differ with respect to the fraction of the twinning shear involved. It is found [II-(9.8)] that 0.4077 of the twinning shear is involved in the $(\alpha+, \omega+)$-solution, while the other solution involves the fraction 0.5923. It is reasonable to suppose that the twin orientation is less favoured because of the larger fraction of the twinning shear that is involved in its formation.

The only experimental data which remain to be considered concern the magnitude and direction of the homogeneous strain. According to the theory

*The six-figure accuracy is needed to obtain self-consistent numerical results.

(II-§9) this strain is represented when referred to the basis F by the matrix

$$(6.2) \qquad (\mathrm{F}\mathbf{p}_1\mathrm{F}) = \mathbf{I} + m\,\mathbf{dp}',$$

where

$$(6.3) \quad -\mathbf{d} = [0.21017, 0.61850, -0.75715]_{\mathrm{F}},$$

$$(6.4) \quad \mathbf{p}' = (0.18726, 0.55102, 0.81321)_{\mathrm{F}},$$

represent unit vectors parallel to the direction of the strain and the normal to the habit plane respectively, and

$$(6.5) \qquad m = 0.19144,$$

is the magnitude (I-§5) of this strain.

In their analysis of this strain, Greninger and Troiano assumed it to be a simple shear on the habit plane, and determined the shear direction as the intersection of the habit plane with a plane defined by direction of a specimen edge before and after transformation. If the theory is correct all such planes should intersect along the predicted direction (6.3). The observed scatter of Greninger and Troiano's shear direction is just that expected, provided all specimen edges studied were within about 60° of the normal to the habit plane. The direction of their trial shear "A" is about 1° from the projection of the predicted direction on the habit plane. The measured angles of shear range from 8° to 14° with a mean of about 11° which compares favourably with the prediction that the direction normal to the habit plane rotates by 11.0°. Thus, the theory is not inconsistent with these observations.

7. Machlin and Cohen's (259)-Transformation

Machlin and Cohen's [14] analysis of the transformation in Fe–30% Ni is the most recent measurement of the homogeneous strain accompanying the transformation. The predictions of the theory for this case are summarized below using $\gamma = 1$ and $\theta^2 = 0.647$.

The invariant line strain for α and ω positive now becomes

$$(7.1) \quad (\mathrm{LSL}) = \begin{pmatrix} 1, & -0.093129, & 0.308397 \\ 0, & 1.114712, & 0.016826 \\ 0, & 0.115080, & 0.935472 \end{pmatrix},$$

and $\cos\alpha = 0.301977$. The angle between $[1\bar{1}0]_{\mathrm{F}}$ and $[11\bar{1}]_{\mathrm{B}}$ is now 3.1°, while the angle between $(111)_{\mathrm{F}}$ and $(101)_{\mathrm{B}}$ is 24′. This orientation relationship is about ½° nearer the Nishiyama relationship than the previous one (§6). No precision determination of the orientation relationship has been made but the predicted orientation does lie within the scatter of the results obtained by the pole figure method [6; 15].

The homogeneous strain is given by an expression of the form (6.2) where

$$(7.2) \quad -\mathbf{d} = [0.23008, 0.63891, -0.73407]_{\mathrm{F}},$$

$$(7.3) \quad \mathbf{p}' = (0.20226, 0.56166, 0.80227)_{\mathrm{F}},$$

$$(7.4) \quad m = 0.22254,$$

while the inhomogeneous shear is 0.4031 of the twinning shear. Machlin and Cohen estimate that the homogeneous strain has a shear component of 0.20 and a component normal to the habit plane of 0.05; the corresponding values predicted by the theory are 0.219 and 0.041.

In comparing the predicted direction (7.2) with Machlin and Cohen's observations, it must be remembered that they were only able to measure the projection of the direction on the $(111)_{\mathrm{F}}$-plane. In Figure 8, their measured direction is compared

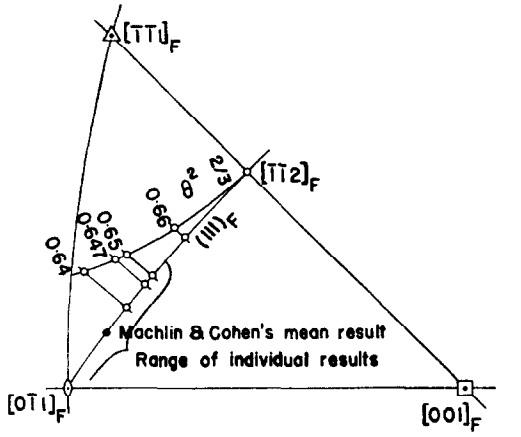

FIGURE 8. Stereographic projection showing the predicted variation (for $\gamma = 1$) of the direction of the homogeneous strain. The projection of this direction on the $(111)_{\mathrm{F}}$-plane is compared with Machlin and Cohen's results.

with the projection of the predicted direction on this plane. The direction given by Machlin and Cohen is a mean of all their results. Since the scatter of their individual measurements is conservatively estimated, from the data in their Table I*, to be ±10° the agreement between theory and experiment is reasonable. The predicted direction is about 5° out of the $(111)_{\mathrm{F}}$-plane which is consistent with the errors stated in Machlin and Cohen's paper [16].

The scatter of the habit planes determined by Machlin and Cohen (Fig. 7) corresponds to the range of θ^2 from 0.64 to 0.66. The use of the value

*The projection of **d** on the $(11\bar{1})_{\mathrm{F}}$-plane is $[t_{xz}/t_{yz}, 1, 0]$ referred to axes in the directions $[\bar{1}12]_{\mathrm{F}}$, $[1\bar{1}0]_{\mathrm{F}}$, $[111]_{\mathrm{F}}$.

$\theta^2 = 0.647$ in the above comparisons is not of particular significance because the corresponding range of predicted directions lies almost entirely within the scatter of the experimental results (Fig. 8). If the scatter of the habit planes is real, it will be necessary to make measurements on individual martensite plates and then, perhaps, it may be possible to distinguish between the present hypothesis and those for which the complementary strain is either on the twinning plane or in the twinning direction.

8. The (225)-Transformations

In iron-carbon alloys containing less than 1.4% carbon the habit planes all contain a close-packed direction $\langle 110\rangle_F$. Above 0.9%-carbon the habit planes are in the vicinity of $(225)_F$ (see Fig. 5), but as the carbon content is lowered below 0.9% the martensite plates degenerate first into laths and then into needles. Although the habit planes have not been determined in these cases the long axes of the crystals are in $\langle 110\rangle_F$ directions. Accordingly in applying the theory to these transformations θ^2 is taken to have its maximum value. Thus, $\alpha = 90°$ and the invariant line is parallel to the twinning direction $[110]_F$ or $[11\bar{1}]_B$. Equation (4.10) for (LSL) now simplifies somewhat and it can readily be shown that the $(\alpha+, \omega+)$- and $(\alpha+, \omega-)$-solutions represent the same strain; similarly, for the other pair. Remembering the relations between solutions described in section 4, it follows that the variants are twin related in pairs. Hence, this group of transformations is a degenerate case of the general theory.

Since $[1\bar{1}0]_F$ and $[11\bar{1}]_B$ are now always parallel, the orientation relationships can be described conveniently by the angle ψ between the planes $(111)_F$ and $(101)_B$. The angle ψ increases as the pole $(101)_B$ moves from $(111)_F$ towards $(001)_F$ and is given by

$$\psi = \omega + \xi - \eta, \tag{8.1}$$

where ω is the angle (equation (4.11)) between $(110)_F$ and $(112)_B$, ξ the angle between $(101)_B$ and $(112)_B$, and η the angle between $(111)_F$ and $(110)_F$. Thus,

$$\left.\begin{aligned} \sin\omega &= (2-\gamma^2)^{\frac{1}{2}}[(2+\gamma^2)^{\frac{1}{2}} - \sqrt{2}\gamma]/2(2+\gamma^2)^{\frac{1}{2}}, \\ \sin\xi &= \gamma/\sqrt{2}(1+\gamma^2)^{\frac{1}{2}}, \\ \sin\eta &= 1/\sqrt{3}, \end{aligned}\right\} \tag{8.2}$$

and the calculated variation of ψ with γ is shown in Figure 9. The predicted orientation relationship is exactly that of Kurdjumow-Sachs for $\gamma = 1$ and never differs from it by more than about 15′. This is in agreement with the pole figure determinations of Kurdjumow-Sachs [3] and of Wassermann [17].

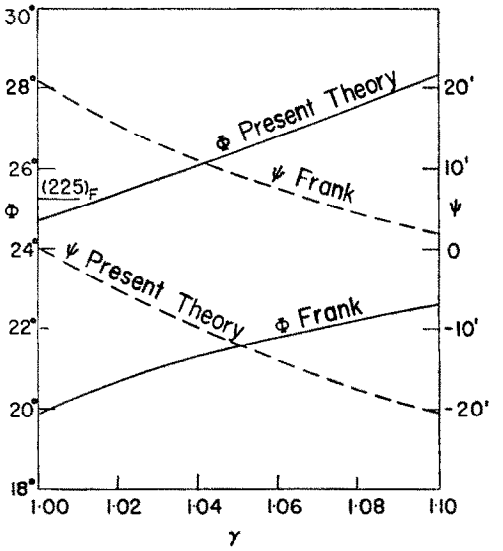

FIGURE 9. Comparison of the predictions of the present theory with that of Frank. Φ is the angle between the habit plane and $(111)_F$, and ψ the angle between the planes $(111)_F$ and $(101)_B$.

The homogeneous strain is given by an expression of the form (6.2) where

$$-\mathbf{d} = [(2-\gamma^2)^{\frac{1}{2}}, (2-\gamma^2)^{\frac{1}{2}}, -2\gamma]_F/\sqrt{2}(2+\gamma^2)^{\frac{1}{2}} \equiv [11\bar{2}]_F, \text{ for } \gamma = 1, \tag{8.3}$$

$$\mathbf{p}' = ((2-\gamma^2)^{\frac{1}{2}}, (2-\gamma^2)^{\frac{1}{2}}, \sqrt{2}(2+\gamma^2)^{\frac{1}{2}})_F/2\sqrt{2}, \equiv (2, 2, 4.90)_F, \text{ for } \gamma = 1, \tag{8.4}$$

$$m = 2[(2+\gamma^2)^{\frac{1}{2}} - \sqrt{2}\gamma]/(2+\gamma^2). \tag{8.5}$$

The inhomogeneous shear is always one-half of the twinning shear. It follows that twin orientations with same habit plane are produced equivalently and are therefore variants as stated above.

The above predictions for this special case are exactly the same as those obtained by Bowles [5] but differ somewhat from those of Frank [18]. Frank suggested that the habit plane is determined by the condition that the close-packed planes $(111)_F$, $(101)_B$ meet edge to edge in the habit plane. This is automatically true in the present theory provided that the $(111)_F$-plane intersects the habit plane (and the twinning plane) along the invariant line $[1\bar{1}0]_F$. This condition is satisfied in the present case ($\alpha = 90°$) but will not always hold, so that Frank's theory cannot be extended to more general cases.

The predictions of the two theories are compared

in Figure 9. The angle ψ (equation (8.1)) between the planes $(111)_F$ and $(101)_B$ is defined in the same way as in Frank's paper, while his angle ϕ between $(111)_F$ and the normal to the habit plane is here denoted by Φ and, on the present theory, is given by

$$\cos \Phi = [\sqrt{2}(2 - \gamma^2)^{\frac{1}{2}} + (2 + \gamma^2)^{\frac{1}{2}}]/2\sqrt{3}. \quad (8.6)$$

The curves labelled "Frank" have been computed from the equations in §-7 of Frank's paper using the uncorrected parameters given therein. The habit planes so predicted are clearly incompatible with observation. To improve the agreement Frank has suggested that before applying the theory the experimental lattice parameters should be adjusted so that the atoms in the $[1\bar{1}0]_F$, $[11\bar{1}]_B$ rows match. One way of doing this is to change all the parameters of one structure by the same factor; this is equivalent to the introduction of the dilatation δ in the present theory. When this is done the two theories give the same result. Frank employed a different method of correction but apparently applied the correction in the wrong sense for his procedure leads to even worse agreement with observation.

In the development of his theory Frank has taken as clues the parallelism of the close-packed directions $[1\bar{1}0]_F$, $[11\bar{1}]_B$, and the close parallelism of the close-packed planes $(111)_F$, $(101)_B$. He envisages a simple type of interface in which these planes meet edge to edge along these directions. In the development of the present theory the authors have argued (Part I) that twinning is of fundamental significance. The twinning plane $(112)_B$ is generated from $(110)_F$ and since, in the present theory, these planes always intersect along the invariant line they necessarily meet edge to edge in the interface in all cases. The agreement between the two theories for $(225)_F$-transformations stems from the coincidence that in these transformations the invariant line is $[1\bar{1}0]_F$ which also lies in the plane $(111)_F$.

9. Discussion

The general conclusion to be drawn from the preceding analysis of specific transformations is that the theory is in substantial agreement with the available experimental data, although this data is inadequate for a conclusive test. To distinguish between the present hypothesis and the alternative ones where the complementary shear is either on the twinning plane or in the twinning direction, measurements of properties such as the habit plane, orientation relationship, direction and magnitude of the homogeneous strain, will have to be made on individual martensite plates.

The present hypothesis provides a description of the overall atomic displacements produced by a transformation, which is certainly very nearly correct. If it is correct, the problem of finding suitable mechanisms for these transformations is reduced to discovering those which are compatible with the hypothesis; any such mechanism would automatically be consistent with all the geometrical properties of the transformations. It seems almost certain that a satisfactory mechanism will involve the motion of dislocations and the theory suggests that these dislocations will be related in some way to twinning in the final structure.

The theory contains one adjustable parameter, δ, which has been estimated from the observed habit plane. It may be asked what physical or geometrical requirement determines its value. If the requirement were purely geometrical, it might be hoped that its nature would emerge from a study of the transformations as a whole. Although this has not proved to be the case, an interesting feature of the iron-carbon group of transformations has been noticed and may be of some significance.

The habit planes observed in iron-carbon alloys containing 0–1.78% carbon are plotted in Figure 10, together with the predicted variation of the habit plane, for $\beta = 54° 44'$ ($\cos \beta = 1/\sqrt{3}$), and $\beta = 56° 20'$.* Along these latitude circles the

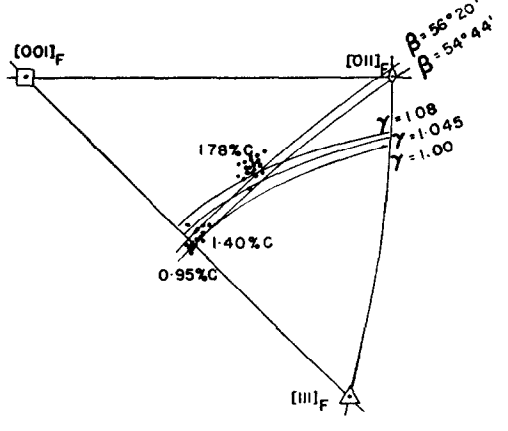

FIGURE 10. The same as figure 5, together with the lines along which β takes the values 54° 44′ and 56° 20′.

*For $\alpha = 90°$, $\tan (54° 44' - \Phi) = \cos \beta$, and then these values of β correspond to habit planes 30° and 29° from $(001)_F$ respectively.

angle ψ between the close-packed planes is zero and approximately 7′ respectively. Although the data is inadequate, it is in agreement with a requirement that as the carbon content increases ψ increases to about 7′ and thereafter remains approximately constant. As γ increases the transformations can be of the $(225)_F$-type until ψ reaches 7′; thereafter, the habit plane would move rapidly out into the centre of the triangle along the line $\beta = 56° 20'$, for the lines γ = const. cross the lines β = const. at a small angle. Such a rapid change of habit plane with γ could account for the reported discontinuous variation of the habit plane at 1.4% carbon [19].

Another feature of interest is that the latitude circle corresponding to $\cos \beta = 1/\sqrt{3}$ and $\psi = 0$, passes through $(011)_F$. If this latitude circle has any particular significance one might expect that a transformation with γ about $\sqrt{2}$ would have a habit plane in the neighbourhood of $(011)_F$. This is the case for transformations such as In-Tl [20; 21] or Cu-Mn [22]. These transformations are special cases of the present class.

References

1. Bowles, J. S. and Mackenzie, J. K. Acta Met. **2** No. 1 (1954). p. 129.
2. Jaswon, M. A. and Wheeler, J. A. Acta Cryst. **1** (1948) 216.
3. Kurdjumow, G. and Sachs, G. Z. Phys. **64** (1930) 325.
4. Lyman, T. Discussion to N. J. Petch. J. Iron Steel Inst. **147** (1943) 221.
5. Bowles, J. S. Acta Cryst. **4** (1951) 162.
6. Nishiyama, Z. Sci. Rep. Tohoku Univ. **23** (1934–35) 638.
7. Greninger, A. B. and Troiano, A. R. Trans. Amer. Inst. Min. (Metall.) Engrs. **185** (1949) 590.
8. Roberts, C. S. J. Metals **5** (1953) 203.
9. Owen, E. A., Yates, E. L. and Sully, A. H. Proc. Phys. Soc. **49** (1937) 315.
10. Bradley, A. J., Jay, A. H. and Taylor, A. Phil. Mag. **23** (7) (1937) 547.
11. Jette, E. R. and Foote, F. Trans. Amer. Inst. Min. (Metall.) Engrs. **120** (1936) 259.
12. Phragmén, G. J. Iron Steel Inst. **123** (1931) 465.
13. Barrett, C. S. Structure of Metals (New York, McGraw-Hill, 1943).
14. Machlin, E. S. and Cohen, M. J. Metals **3** (1951) 1019.
15. Mehl, R. F. and Derge, G. Trans. Amer. Inst. Min. (Metall.) Engrs. **105** (1937) 215.
16. Bowles, J. S. and Mackenzie, J. K. J. Metals **4** (1952) 1201.
17. Wassermann, G. Mitt. K. Wilh. Inst. Eisenforsch. **17** (1935) 149.
18. Frank, F. C. Acta Met. **1** (1953) 15.
19. Greninger, A. B. and Troiano, A. R. Trans. Amer. Inst. Min. (Metall.) Engrs. **140** (1940) 307.
20. Guttman, L. Trans. Amer. Inst. Min (Metall.) Engrs. **188** (1950) 1472.
21. Bowles, J. S., Barrett, C. S. and Guttman, L. Trans. Amer. Inst. Min (Metall.) Engrs. **188** (1950) 1478.
22. Christian, J. W. and Basinski, Z. S. J. Inst. Metals **80** (1952) 659.